Origin of Atomic Resolution on Metal Surfaces in Scanning Tunneling Microscopy

C. Julian Chen

IBM Research Division, Thomas J. Watson Research Center, P.O. Box 218, Yorktown Heights, New York 10598

(Received 7 November 1989)

Scanning tunneling microscopy has repeatedly resolved individual atoms on a number of metal surfaces with atomic distances 2.5–3 Å. This is in sharp contradiction to the resolution limits previously predicted, 6–9 Å. We present a theory of such atomic resolution in terms of *actual* tip states, for example, d_{z^2} tip states on tungsten tips. Quantitative interpretation of the observed images is obtained with no adjustable parameters. We predict that to achieve atomic resolution, the tip material should be either a *d*-band metal or certain semiconductor.

PACS numbers: 61.16.Di, 61.50.Em

Scanning tunneling microscopy (STM) has repeatedly resolved individual atoms at low Miller index metal surfaces,[1-4] such as Au(111), Al(111), and Cu(100), with nearest-neighbor atomic distances 2.5–3 Å, as shown in Table I. This is in sharp contradiction to the STM resolution limits previously predicted.[5,6] According to the *s*-wave tip model, on metals, only superstructures of reconstructed surfaces with periodicity greater than 6 Å can be resolved.[5] In Lang's numerical simulation of STM images,[6] both tip and sample are modeled as a structureless jellium surface with an extra metal atom adsorbed. The simulated image of that metal atom appeared as a pancakelike protrusion[6] of diameter $\simeq 9$ Å and maximum height $\simeq 1.6$ Å. In other words, both models concluded with no atomic resolution on close-packed metal surfaces.[5,6] Facing this controversy, some authors propose models of STM imaging based on *mechanical interactions* between tip and sample.[3,7] However, none of these mechanical models provide a consistent explanation of all experimental facts.[7,8]

The *s*-wave tip model fails in explaining the observed atom-resolved images because it models the tip as a *macroscopic continuum,*[5] i.e., a potential well with local radius of curvature R. With $R = 9$ Å and a tip-sample distance 15 Å, at low bias, Tersoff and Hamann show that the center of curvature of the tip follows the contour of the Fermi-level local density of states (LDOS) of the sample.[5] "In any case," they emphasized,[5] "the *s*-wave treatment here is not intended as an accurate description of a real tip, but rather as a useful way of parametrizing the effect of finite tip size." Clearly, to account for the observed atom-resolved images, the actual electronic states of a real tip should be considered.

TABLE I. Atom-resolved images of metal surfaces by scanning tunneling microscopy.

Surface	Atomic spacing (Å)	Method	Corrugation (current variation)	Reference
Au(111)	2.87	Current	(10%)	1
Au(111)	2.87	Topographic	0.15 Å	2
Al(111)	2.88	Topographic	0.1–0.8 Å	3
Cu(100)	2.55	Topographic	0.2 Å	4

In this Letter, we present a theory of STM imaging mechanism in terms of actual electronic states on real tips, exemplified by a quantitative explanation of the observed images of close-packed metal surfaces.[3] All commonly used tip materials, W, Pt, and Ir, are *d*-band metals.[9] In the reported experiments,[1-4] tungsten tips are used. At the Fermi level, 85% of its density of states comes from *d* states.[9] Tungsten has a strong tendency to form highly localized metallic d_{z^2} dangling bonds on its surfaces, which is well established both experimentally and theoretically.[10] Cluster calculations[11] confirmed this conclusion: On the apex atom of either W_4 or W_5, there is a localized d_{z^2} state near the Fermi level.[11] Thus, it is reasonable to expect such localized metallic d_{z^2} states to exist on tungsten tips.

Figure 1 shows a qualitative explanation of the effect of a d_{z^2} tip state in the light of the *reciprocity principle* in STM: Upon interchanging the tip state and the sample state, the image should be identical.[12] For an *s*-wave tip state, the STM image of a metal surface is the charge-density contour, which can be evaluated using

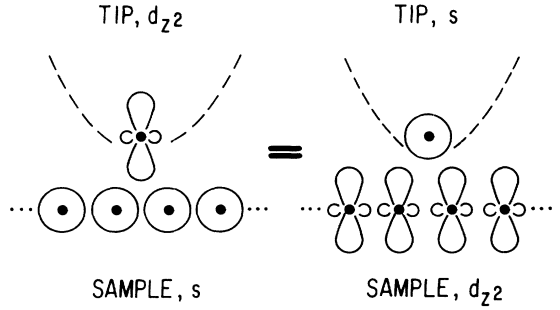

FIG. 1. An intuitive picture of the STM imaging mechanism in terms of a d_{z^2} tip state, in the light of the reciprocity principle (Ref. 12).

atomic-charge superposition, i.e., as a sum of the charge densities of individual atoms, each made of s states.[5] According to the reciprocity principle (Fig. 1), with a d_{z^2} tip state, the tip no longer traces the charge-density contour of the sample. Instead, it traces the charge-density contour of a *fictitious surface* with a d_{z^2} state on each atom. Obviously, these contours exhibit much stronger atomic corrugation than that of the charge density. The possible role of such a localized d_{z^2} dangling-bond state at the tip was also discussed by Baratoff.[13]

In the following, we present a quantitative analysis of the images of close-packed metal surfaces using the three-dimensional tunneling theory outlined in Ref. 12.

Figure 2 shows the geometry of close-packed metal surface and its surface Brillouin zone.[14] The charge density should have the same symmetry as the surface structure. Neglecting the underlying layers, the charge density should have a hexagonal symmetry, i.e., invariant with respect to plane group $p6mm$ (see Fig. 2). Up to the lowest nontrivial Fourier components, the most general form of surface charge density with a hexagonal symmetry is

$$\rho(\mathbf{r})=\sum_{E\le E_F}|\psi(\mathbf{r})|^2\simeq a_0(z)+a_1(z)\phi^{(6)}(k\mathbf{x}), \quad (1)$$

where $\mathbf{x}=(x,y)$ and $k=4\pi/\sqrt{3}a$ is the length of a primitive reciprocal-lattice vector (see Fig. 2). A hexagonal cosine function is defined for convenience,

$$\phi^{(6)}(\mathbf{x})\equiv\tfrac{1}{3}+\tfrac{2}{9}\sum_{j=0}^{2}\cos(\boldsymbol{\omega}_j\cdot\mathbf{x}), \quad (2)$$

where $\boldsymbol{\omega}_0=(0,1)$, $\boldsymbol{\omega}_1=(-\frac{1}{2}\sqrt{3},-\frac{1}{2})$, and $\boldsymbol{\omega}_2=(\frac{1}{2}\sqrt{3},-\frac{1}{2})$, respectively. It is easy to show that the function $\phi^{(6)}(k\mathbf{x})$ has maximum value 1 at each atomic site, and minimum value 0 at the center of each atomic triangle.

To account for the lowest nontrivial Fourier components of surface charge density, it is sufficient to consider the Bloch functions in the vicinity of several high-symmetry points on the surface Brillouin zone.[15] The $a_0(z)$ term in Eq. (1) comes mainly from the Bloch functions near $\bar{\Gamma}$, whose lowest Fourier component is[15]

$$\psi_{\bar{\Gamma}}\sim\exp(-\kappa z), \quad (3)$$

where the decay constant κ is determined by the work function ϕ through the relation $\kappa=(2m_e\phi)^{1/2}/\hbar\simeq 0.51\sqrt{\phi}$, in Å and eV. This group of Bloch functions contributes to the first term in Eq. (1):

$$a_0(z)\propto\exp(-2\kappa z). \quad (4)$$

The contribution to the second term of Eq. (1) comes from Bloch functions near the $\bar{K}$ points.[15] In general, a surface Bloch function at that point has the form

$$\psi_{\bar{K}}=\exp(i\mathbf{k}_1\cdot\mathbf{x})\sum_{\mathbf{G}}a_{\mathbf{G}}\exp[-(\kappa^2+|\mathbf{k}_1+\mathbf{G}|^2)^{1/2}z]\times\exp(i\mathbf{G}\cdot\mathbf{x}), \quad (5)$$

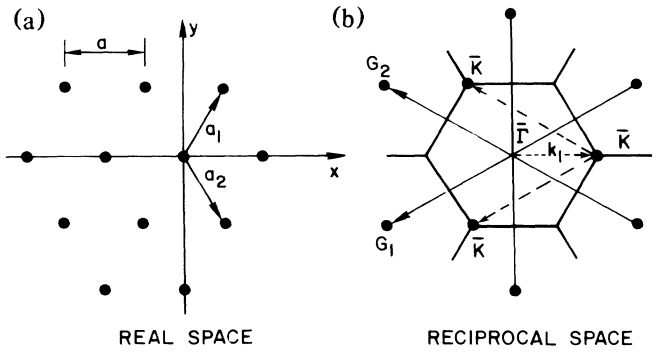

FIG. 2. (a) Geometrical structure of a close-packed metal surface. As shown, the top layer exhibits a sixfold symmetry, which is invariant with respect to plane group $p6mm$, i.e., point group C_{6v} together with the translational symmetry. (b) The corresponding surface Brillouin zone (Ref. 14). The lowest nontrivial Fourier components of LDOS arise from Bloch functions near the $\bar{\Gamma}$ and $\bar{K}$ points. (The symbols for plane groups are explained in, e.g., Ref. 22.)

with $|\mathbf{k}_1|\equiv k_1=k/\sqrt{3}$. By inspecting Eq. (5) and Fig. 2, one finds that the only slow-decaying symmetric Fourier sum of the Bloch functions near $\bar{K}$ is

$$\psi_{\bar{K}}\sim\exp(-\kappa_1 z)\sum_{j=0}^{2}\cos(k_1\boldsymbol{\Omega}_j\cdot\mathbf{x}), \quad (6)$$

where $\boldsymbol{\Omega}_0=(1,0)$, $\boldsymbol{\Omega}_1=(-\frac{1}{2},\frac{1}{2}\sqrt{3})$, $\boldsymbol{\Omega}_2=(-\frac{1}{2},-\frac{1}{2}\sqrt{3})$, and $\kappa_1=(\kappa^2+k_{\parallel}^2)^{1/2}$ is the corresponding decay constant. The charge density is proportional to $|\psi_{\bar{K}}|^2$. Combining with Eq. (4), the total charge density is then

$$\rho(\mathbf{r})\propto\sum_{E\le E_F}|\psi(\mathbf{r})|^2=C_0e^{-2\kappa z}+C_1e^{-2\kappa_1 z}\phi^{(6)}(k\mathbf{x}), \quad (7)$$

where C_0, C_1 are constants. For Al(111),[3] $a=2.88$ Å, $\phi=3.5$ eV, it follows that $\kappa=0.96$ Å^{-1}, $\kappa_1=1.74$ Å^{-1}. The corrugation amplitude of the charge-density contour, Δz as a function of z, can be obtained from Eq. (7),

$$\Delta z=(C_1/C_0)(2\kappa)^{-1}e^{-2(\kappa_1-\kappa)z}+O(e^{-4(\kappa_1-\kappa)z}). \quad (8)$$

The ratio C_1/C_0 can be determined by comparing Eq. (8) with the corrugation amplitudes of the charge-density contours obtained from first-principles calculations. For example, from Fig. 3 of Ref. 14, averaged from five contours ranging from 2.5 to 12.5 atomic units, we find $C_1/C_0\simeq 5.7\pm 1.0$.

To calculate the tunneling current, we expand the sample wave function near the nucleus of the apex atom $\mathbf{r}_0$ in terms of spherical harmonics Y_{lm},

$$\psi=\sum a_{lm}i_l(\kappa r)Y_{lm}, \quad (9)$$

where $r=|\mathbf{r}-\mathbf{r}_0|$ and $i_l(\xi)$ is a spherical modified Bessel function.[12] The tunneling matrix element[12] for a d_{z^2} tip state, i.e., $(l=2,m=0)$ tip state, is proportional

to α_{20}. Using the properties of $i_l(\xi)$ and Y_{lm}, it is straightforward to show that

$$M \propto \alpha_{20} \propto \kappa^{-2}\partial^2\psi/\partial z^2 - \tfrac{1}{3}\psi . \tag{10}$$

The values are taken at $\mathbf{r}_0$. As shown, the form of the tunneling matrix elements follows a simple *derivative rule*.[12] For nearly-free-electron metals, the lowest nontrivial Fourier components of Fermi-level LDOS is proportional to those of the charge density. The tunneling current[12] is proportional to $|M|^2$. Comparing with Eq. (7), we find the total tunneling current:

$$I \propto \sum_{E=E_F}^{E_F+eV} |\kappa^{-2}\partial^2\psi/\partial z^2 - \tfrac{1}{3}\psi|^2 \propto C_0(\tfrac{2}{3})^2 e^{-2\kappa z} + C_1(\kappa_1^2/\kappa^2 - \tfrac{1}{3})^2 e^{-2\kappa_1 z}\phi(k\mathbf{x}) . \tag{11}$$

Using the values of κ, κ_1, and C_1/C_0, the corrugation amplitude of the topographic image (in Å) is

$$\Delta z = (C_1/C_0)[\tfrac{3}{2}(\kappa_1^2/\kappa^2 - \tfrac{1}{3})]^2(2\kappa)^{-1} e^{-2(\kappa_1-\kappa)z} + O(e^{-4(\kappa_1-\kappa)z}) \simeq (58 \pm 10)\exp(-1.56z) , \tag{12}$$

which is about 19.6 times greater than the charge-density corrugation, Eq. (8).

A comparison of Eq. (12) with experiments[3] is shown in Fig. 3. The slope of the $\ln\Delta z \sim z$ curve from Eq. (12) fits well with experimental data. The absolute tip-sample distance is obtained from curve fitting, which gives the shortest average tip-sample distance at $I=40$ nA (with bias 50 mV) to be about 2.9 Å. According to a recent first-principles calculation of an Al-Al system,[8] the nucleus-nucleus distance of a mechanical contact is about 2.3 Å. The local tip-sample distance at an atomic site is the average z plus about one-half of the corrugation amplitude. This results in a closest distance $\sim$3.3 Å, which is about 1 Å before a mechanical contact. This is in good agreement with the measured tip-sample separation,[16] about 1 Å before a mechanical contact at tunneling conductance $10^{-6}\ \Omega^{-1}$.

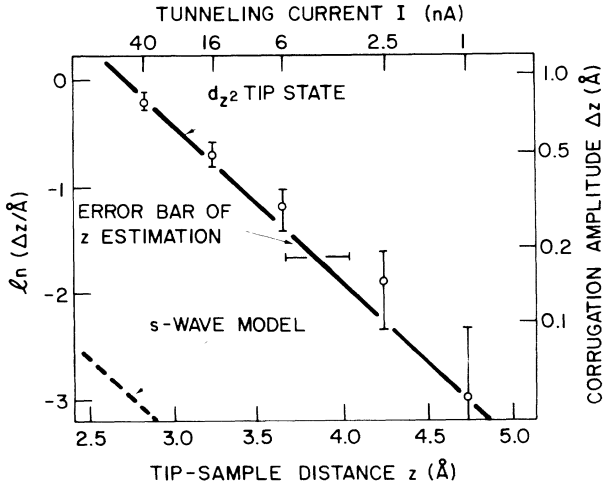

FIG. 3. Interpretation of the atomic resolution observed on Al(111). The predicted corrugation amplitude with a d_{z^2} tip state (solid curve) agrees well with the experimental data from Fig. 2 of Ref. 3 (circles with error bars). The parameters of the theoretical curve are taken from a first-principles calculation of Al(111) surface, Ref. 14. The tip-sample distance is defined as the distance from the plane of the top-layer nuclei of the sample to the center of the apex atom of the tip. That shortest distance, obtained from curve fitting, agrees well with direct measurements, Ref. 16. The corrugation predicted by the s-wave model (dashed curve), that is, the corrugation of Fermi-level LDOS contour (Ref. 5), is included for comparison.

An interpretation of the tip-treatment procedure described in Ref. 3 is as follows. As reported, by applying a bias of about -7.5 V on the sample for a while, the tip withdrew by $\sim$25 Å. After that, atomic resolution was achieved.[3] Actually, the W atoms on the tip surface, surrounded with a thinner electron density than that in the bulk, experience a reduced force from the electron wind as comparing with those in the bulk.[17] The W atoms on the tip surface thus exhibit a net positive charge. The electrical field attracts the W atoms on the tip surface towards the apex. As a result, a W cluster is formed often with a single atom at its apex, which gives rise to a metallic d_{z^2} tip state.[10,11] This explanation is in agreement with a recent electron-microscopy study of the electromigration of W atoms on W tips.[18]

The localized metallic surface state on the tip is essential in STM for achieving atomic resolution.[13,19] Besides free-electron metals, atomic resolution (2–4 Å) has been observed on semiconductors[19] and metallic layered materials.[20] For example, on MoS_2, atoms with spacing 1.3 Å are clearly resolved.[21] However, atomic resolution occurs only with an infrequent "good tip."[1-4,19-21] Even on reconstructed surfaces, for example, Si(111)7×7 and Si(111)$\sqrt{3}\times\sqrt{3}$-Al, with an atomic spacing $\sim$7 Å, the observed corrugation amplitudes and the slopes dz/dx can be much greater than the predictions of the s-wave model.[19] It was proposed that the tip may pick up a Si cluster from Si surface to form a p_z dangling bond on the tip, and atomic resolution is resumed.[19] The STM image from a p_z tip state can be calculated using a method similar to that for a d_{z^2} tip state.[12]

The early STM theories asserted that the STM resolution was independent of tip material.[5] As we have shown, atomic resolution in STM requires localized metallic p_z or d_{z^2} tip states. Therefore, as tip materials, only d-band metals[9] (for example, Pt, Ir, W) and semiconductors that tend to form p_z-like metallic dangling bonds (for example, silicon[19]) may provide atomic resolution. A careful experimental study of STM resolution

versus the chemical identity of the apex atom will further clarify the nature of STM imaging mechanism.

In conclusion, we have presented a theory of STM imaging mechanism in terms of localized surface states on the tip, for example, p_z and d_{z^2} dangling-bond states. With these tip states, the nucleus of the apex atom of the tip follows a contour determined by the derivatives of surface wave functions of the sample, which exhibits much stronger atomic corrugation than Fermi-level LDOS. The theory is exemplified by a quantitative interpretation of the observed atom-resolved STM images on close-packed metal surfaces.

The author wishes to acknowledge J. E. Demuth, R. J. Hamers, J. Tersoff, L. D. Lang, I. P. Batra, A. Baratoff, V. Moruzzi, N. Garcia, and H. Rohrer for helpful discussions, S. Chiang and P. Lippel for discussion of unpublished experimental details as well as J. Pethica, S. Ohnishi, and A. Baratoff for sending me unpublished manuscripts.

[1]V. M. Hallmark, S. Chiang, J. F. Rabolt, J. D. Swalen, and R. J. Wilson, Phys. Rev. Lett. **59**, 2879 (1987).

[2]Ch. Wöll, S. Chiang, R. J. Wilson, and P. H. Lippel, Phys. Rev. B **39**, 7988 (1989).

[3]J. Wintterlin, J. Wiechers, H. Burne, T. Gritsch, H. Höfer, and R. J. Behm, Phys. Rev. Lett. **62**, 59 (1989).

[4]P. H. Lippel, R. J. Wilson, M. D. Miller, Ch. Wöll, and S. Chiang, Phys. Rev. Lett. **62**, 171 (1989). The number 0.2 Å in Table I is a private information from the authors.

[5]J. Tersoff and D. R. Hamann, Phys. Rev. Lett. **50**, 1998 (1983); Phys. Rev. B **31**, 805 (1985).

[6]N. D. Lang, Phys. Rev. Lett. **55**, 230 (1985); **56**, 1164 (1986).

[7]J. B. Pethica [Phys. Rev. Lett. **57**, 3235 (1986)] proposed that the observed periodic patterns in STM images are due to the periodic misalignment of atomic planes during sharing under intimate mechanical contact. This model cannot explain the observed atomic-size defects (Ref. 2) and the 3–5-eV apparent barrier height (Ref. 3). For an analysis of the mechanical model proposed in Ref. 3, see S. Ciraci, A. Baratoff, and I. P. Batra, IBM Research Report No. RZ 1882, 1989 (to be published).

[8]Ciraci, Baratoff, and Batra (Ref. 7).

[9]D. A. Papaconstantopoulos, *Handbook of the Structure of Elemental Solids* (Plenum, New York, 1986).

[10]S.-L. Weng, E. W. Plummer, and T. Gustafsson, Phys. Rev. B **18**, 1718 (1978); M. Posternak, H. Krakauer, A. J. Freeman, and D. D. Koelling, Phys. Rev. B **21**, 5601 (1980); L. F. Mattheiss and D. R. Hamann, Phys. Rev. B **29**, 5372 (1984).

[11]S. Ohnishi and M. Tsukuda, Solid State Commun. **71**, 391 (1989).

[12]C. J. Chen, J. Vac. Sci. Technol. A **6**, 319 (1988). Equation (9) in this reference is accurate up to the leading term, which is enough for all discussions therein. The accurate expression of α_{20} has two terms, as shown in the text. Remember that the angular dependence of a d_{z^2} state is $z^2-\frac{1}{3}r^2$ rather than z^2, the accurate expression of the tunneling matrix element for the d_{z^2} tip state agrees well with the "derivative rule" originally shown for $m\neq 0$ tip states.

[13]A. Baratoff, Physica (Amsterdam) **127B**, 143 (1984).

[14]K. Mednick and L. Kleinman, Phys. Rev. B **22**, 5768 (1980).

[15]This approach is well established in the theory of helium scattering, see J. Harris and A. Liebsch, Phys. Rev. Lett. **49**, 341 (1982); A. Liebsch, J. Harris, and M. Weinert, Surf. Sci. **145**, 207 (1984). It was later applied for analyzing STM images on metals, see J. Tersoff and D. R. Hamann, Phys. Rev. B **31**, 807–808 (1985). For further justification of this approach in STM-related problems, a calculation assuming a uniform $\rho(\mathbf{k})$ distribution over the surface Brillouin zone is performed. Very similar results are obtained [C. J. Chen (unpublished)].

[16]U. Dürig, J. K. Gimzewski, and D. W. Pohl, Phys. Rev. Lett. **57**, 2403 (1986); U. Dürig, O. Züger, and D. W. Pohl, J. Microscopy **152**, 259 (1988).

[17]C. Bosvieux and J. Friedel, J. Phys. Chem. Solids **23**, 123 (1962); R. P. Gupta, *ibid.* **47**, 1057 (1986).

[18]H. Neddermeyer and M. Drechsler, J. Microscopy **152**, 459 (1988).

[19]J. E. Demuth, U. Koehler, and R. J. Hamers, J. Microscopy **151**, 299 (1988).

[20]R. V. Coleman, B. Giambattisa, P. K. Hansma, A. Johnson, W. W. McNairy, and C. G. Slough, Adv. Phys. **37**, 559 (1988).

[21]M. Weimer, J. Kramer, C. Bai, and J. D. Baldschmieler, Phys. Rev. B **37**, 4292 (1988).

[22]*International Tables for Crystallography* (Reidel, Dordrecht, 1987), Vol. A.